Supporting Information

Metastable behavior of Noble Gas inserted Tin and Lead Fluorides

Sudip Pan,[1] Ashutosh Gupta,[2] Subhajit Mandal,[1] Diego Moreno,[3] Gabriel Merino*,[3] and Pratim K. Chattaraj*,[1]

[1]*Department of Chemistry and Centre for Theoretical Studies, Indian Institute of Technology, Kharagpur, 721302, India.*
[2]*Department of Chemistry, Udai Pratap Autonomous College, Varanasi, Uttar Pradesh, 221002 India.*

[3] *Departamento de Física Aplicada, Centro de Investigación y de Estudios Avanzados Unidad Mérida. km 6 Antigua carretera a Progreso. Apdo. Postal 73, Cordemex, 97310, Mérida, Yuc., México.*

* Corresponding authors: gmerino@mda.cinvestav.mx
pkc@chem.iitkgp.ernet.in

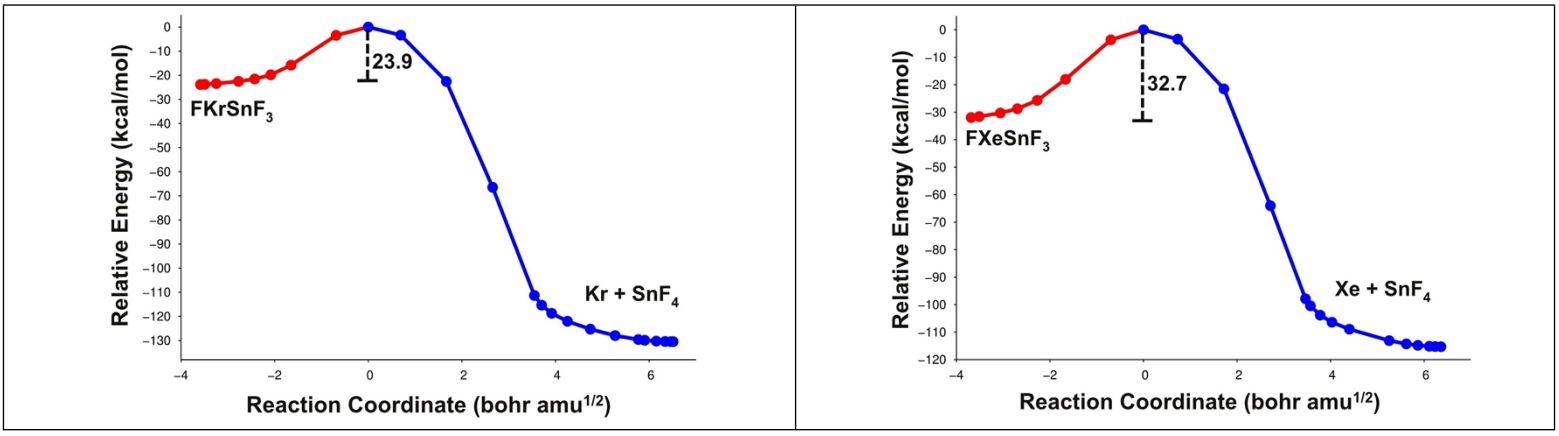

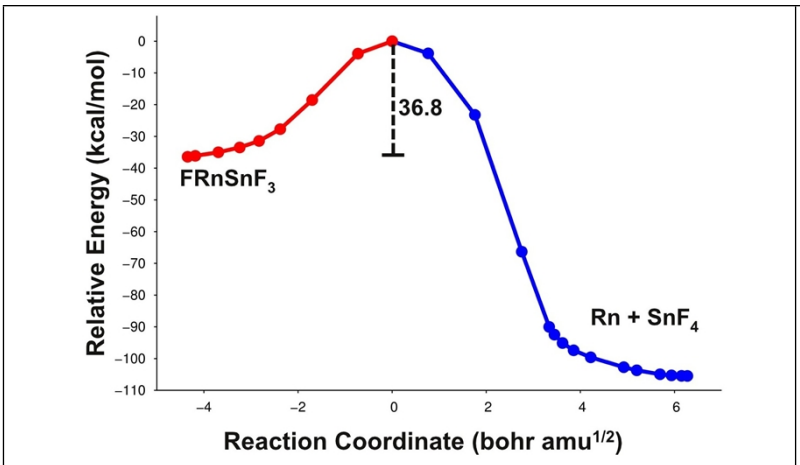
Relative Energy (kcal/mol)
Reaction Coordinate (bohr amu1/2)
FRnSnF3
36.8
Rn + SnF4

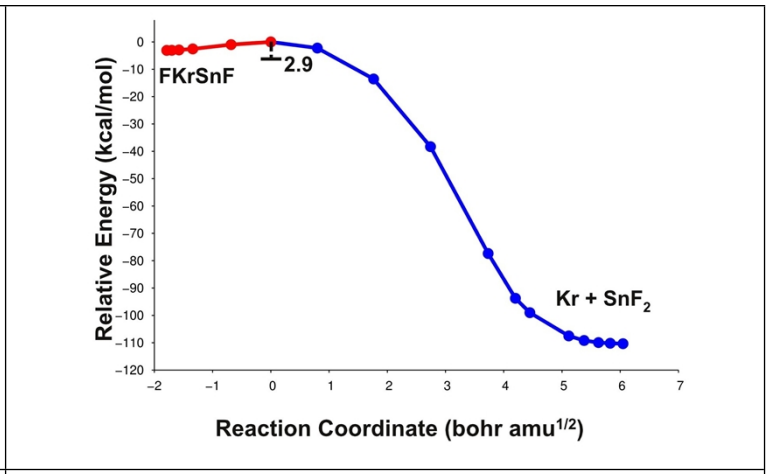
Relative Energy (kcal/mol)
Reaction Coordinate (bohr amu1/2)
FKrSnF
2.9
Kr + SnF2

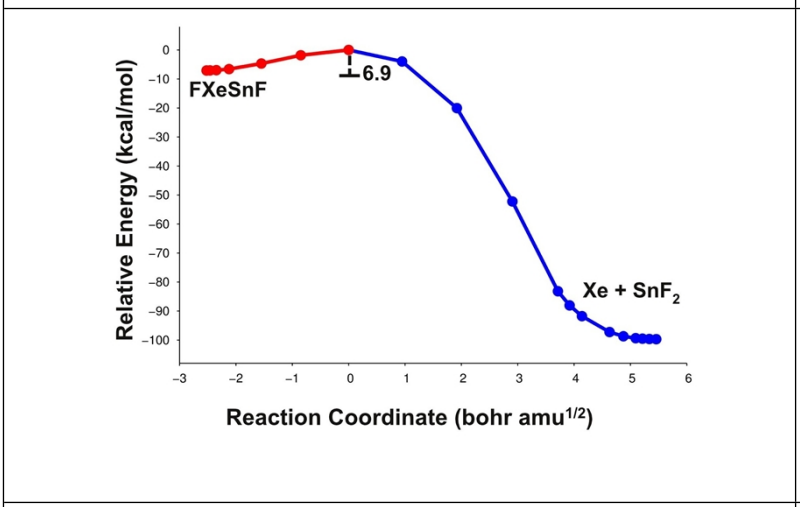
Relative Energy (kcal/mol)
Reaction Coordinate (bohr amu1/2)
FXeSnF
6.9
Xe + SnF2

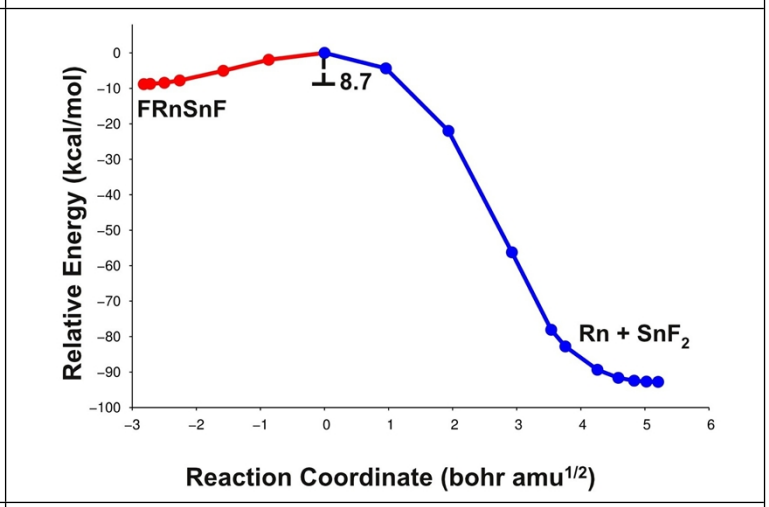
Relative Energy (kcal/mol)
Reaction Coordinate (bohr amu1/2)
FRnSnF
8.7
Rn + SnF2

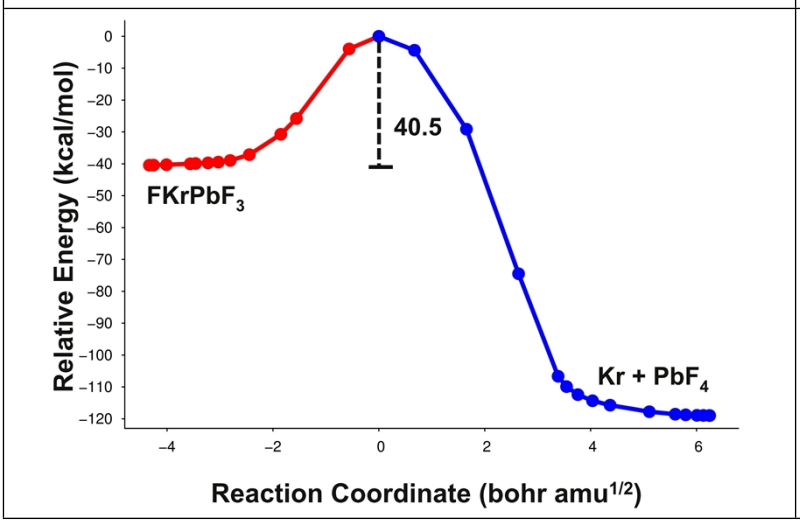
Relative Energy (kcal/mol)
Reaction Coordinate (bohr amu1/2)
FKrPbF3
40.5
Kr + PbF4

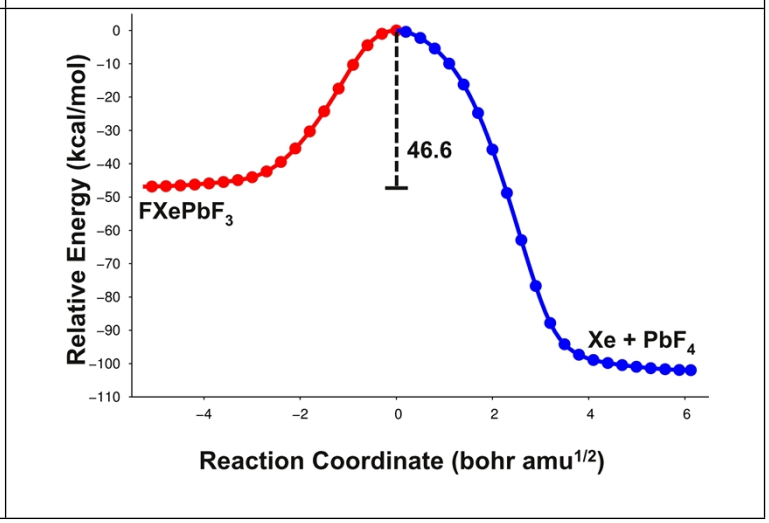
Relative Energy (kcal/mol)
Reaction Coordinate (bohr amu1/2)
FXePbF3
46.6
Xe + PbF4

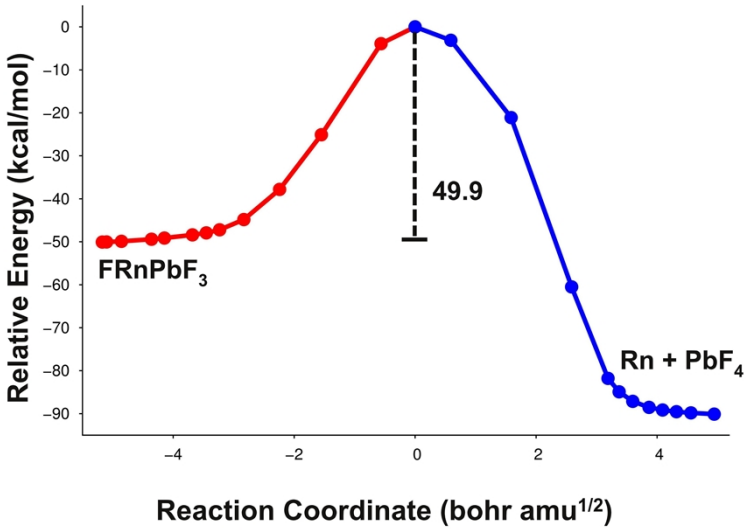

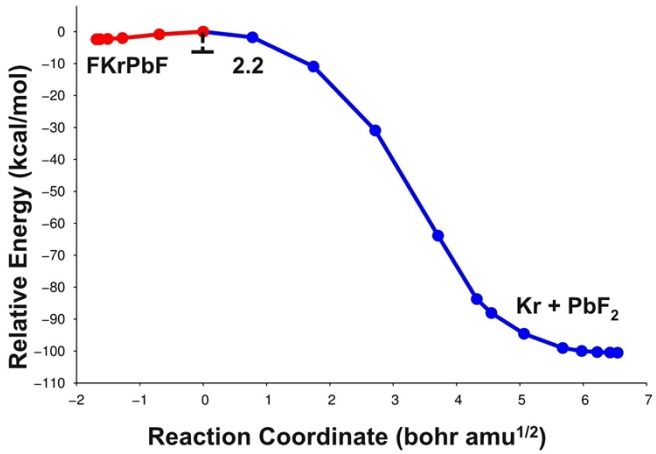

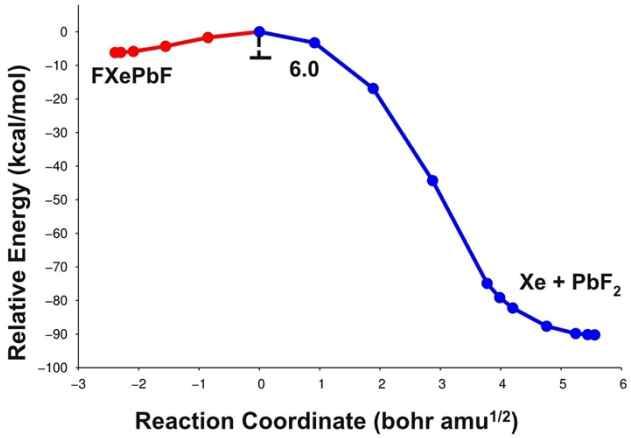

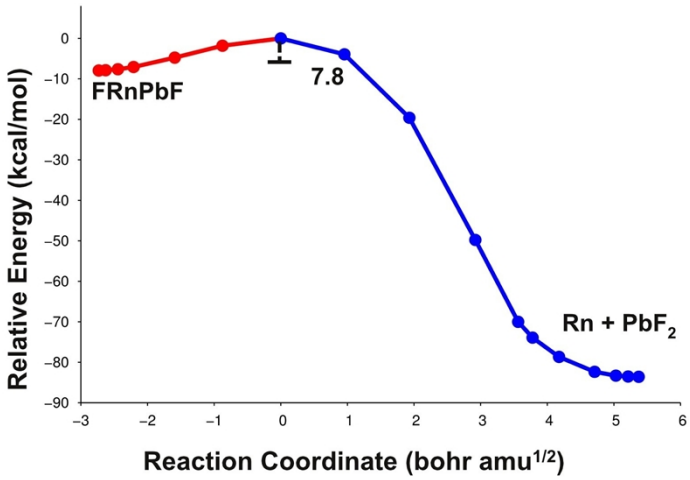

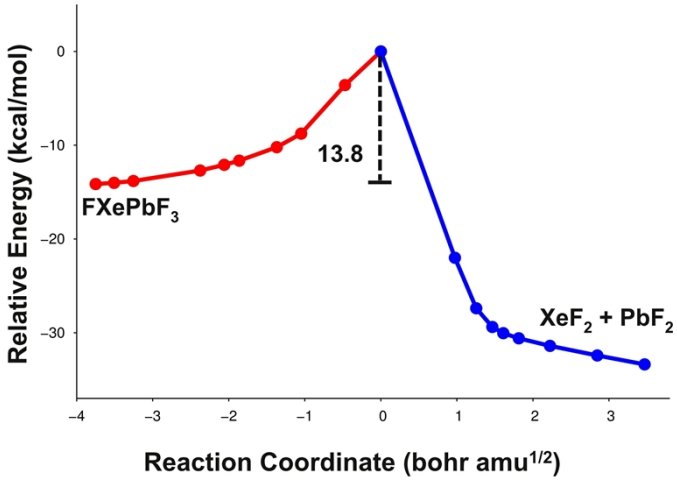

IRC for $FXePbF_3 \rightarrow XeF_2 + PbF_2$

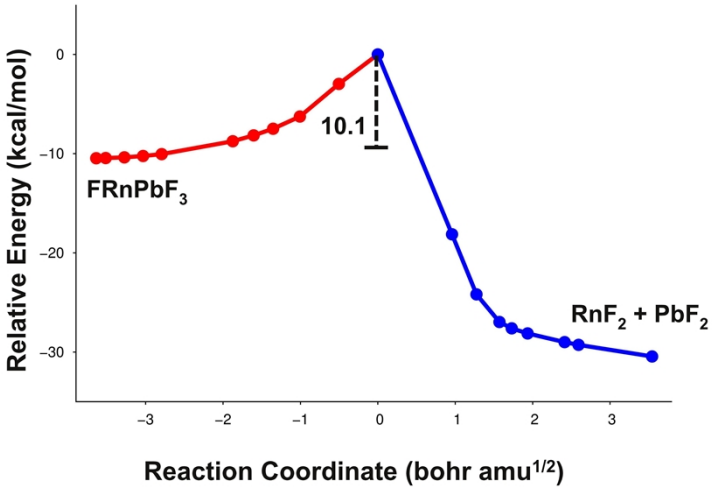

IRC for $FRnPbF_3 \rightarrow RnF_2 + PbF_2$

Fig. S1 The IRC plots for the dissociations of $FNgEF_3$ and FNgEF producing Ng and EF_4 or EF_2. The IRC plots in the last row correspond to the dissociation of $FNgPbF_3$ producing NgF_2 and PbF_2.

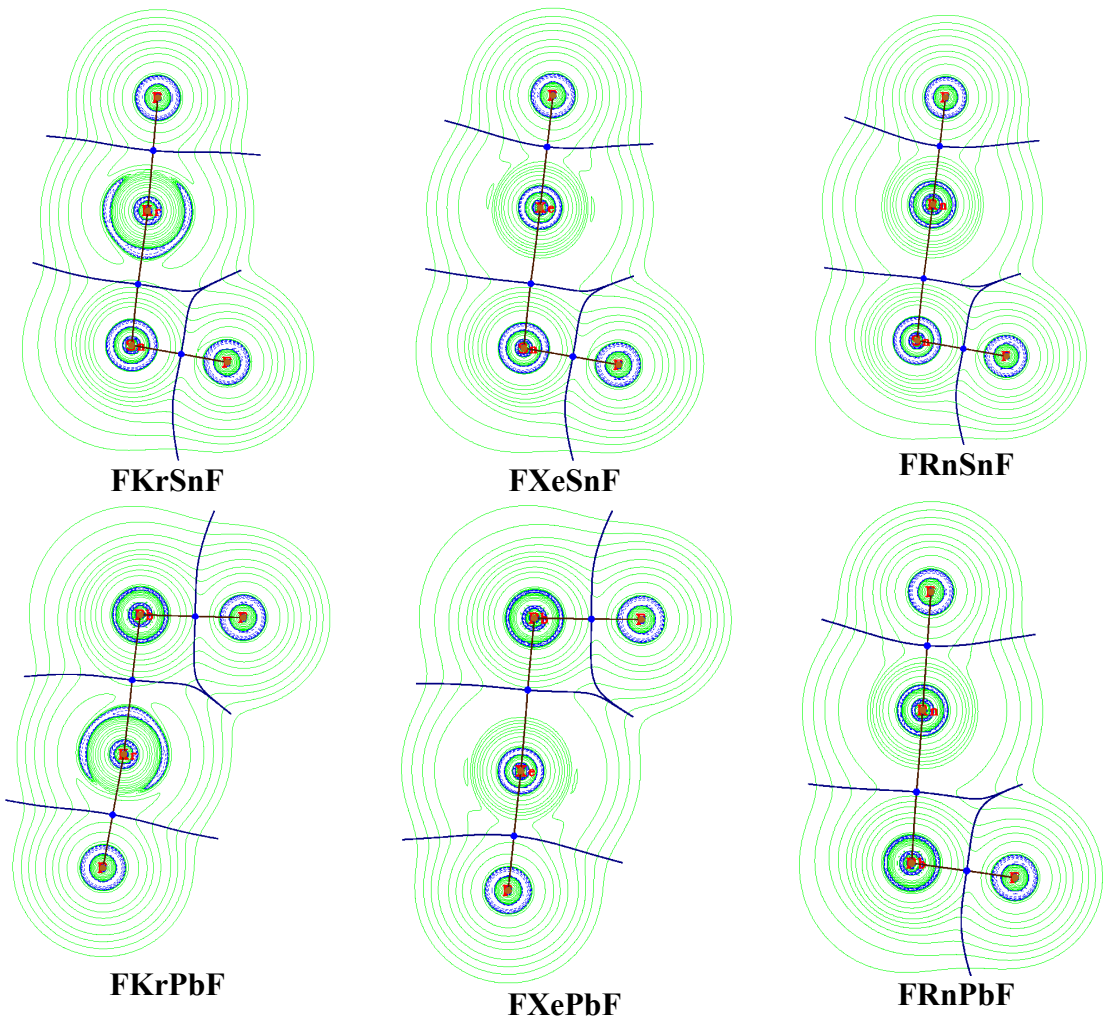

Fig. S2 Contour plots of the Laplacian of the electron density of FNgSnF and FNgPbF clusters at a particular plane computed at the MP2/def2-TZVPPD/WTBS level. (WTBS is used for Sn, Pb, Xe and Rn; Green colored region shows the area of $\nabla^2\rho(\mathbf{r}) > 0$ whereas blue colored region shows the area of $\nabla^2\rho(\mathbf{r}) < 0$)

Table S1. The geometrical parameters (in Å and degree) of the optimized geometries of FNgSnF clusters studied at the CCSD(T)/def2-TZVP level.

	Clusters	r_{F-Ng}	r_{Ng-E}	r_{Sn-F}	<FNgE	<NgEF
Minima	FKrSnF	2.211	2.727	1.915	179.1	93.4
	FXeSnF	2.244	2.892	1.923	179.8[a]	93.4[a]
	FRnSnF	2.283	2.970	1.927	179.6[a]	93.5[a]
	FXePbF	2.259	2.965	2.030	179.0[a]	93.2[a]
	FRnPbF	2.295	3.036	2.035	179.9[a]	93.2[a]

[a]For FXeEF and FRnEF we have fixed the bond angles and dihedral angles as those obtained at the MP2/def2-TZVPPD level to reduce computational time and only bond distances are allowed to vary.

Table S2. The geometrical parameters (in Å and degree) of the optimized geometries of $FNgEF_3$ and FNgEF clusters (both minimum energy structures and transition states) studied at the MP2/def2-TZVPPD level.

	Clusters	r_{F-Ng}	r_{Ng-E}	r_{E-F}	<FNgE	<NgEF
Minimum Energy Structures	$FKrSnF_3$	2.025	2.616	1.890	180.0	111.7
	$FXeSnF_3$	2.102	2.755	1.892	180.0	112.7
	$FRnSnF_3$	2.157	2.827	1.895	180.0	113.3
	FKrSnF	2.241	2.675	1.916	178.2	93.3
	FXeSnF	2.271	2.852	1.926	179.8	93.4
	FRnSnF	2.307	2.930	1.931	179.6	93.5
	$FKrPbF_3$	2.020	2.797	2.009	180.0	114.0
	$FXePbF_3$	2.069	2.852	2.002	180.0	114.8
	$FRnPbF_3$	2.122	2.899	2.002	180.0	115.3
	FKrPbF	2.263	2.753	2.021	176.4	95.2
	FXePbF	2.285	2.921	2.032	179.0	94.3
	FRnPbF	2.317	2.993	2.037	179.9	93.9
Transition States	$FKrSnF_3$	2.332	2.470	1.859, 1.868	109.6	105.9, 106.8
	$FXeSnF_3$	2.384	2.627	1.865, 1.874	101.7	108.0, 108.8
	$FRnSnF_3$	2.424	2.698	1.868, 1.877	96.9	108.9, 109.7
	FKrSnF	2.354	2.648	1.911	126.7	94.3
	FXeSnF	2.399	2.792	1.918	112.0	94.8
	FRnSnF	2.430	2.851	1.921	105.8	95.1
	$FKrPbF_3$	2.351	2.563	1.954, 1.969	105.2	105.6, 106.0
	$FXePbF_3$	2.387	2.698	1.962, 1.975	99.2	108.4, 109.3
	$FRnPbF_3$	2.420	2.757	1.966, 1.979	95.0	109.4, 110.9
	FKrPbF	2.368	2.735	2.017	130.6	97.4
	FXePbF	2.413	2.869	2.024	114.7	96.9
	FRnPbF	2.441	2.921	2.028	108.1	96.7

The transition states correspond to $FNgEF_3 \rightarrow Ng + EF_4$ or $FNgEF \rightarrow Ng + EF_2$.

Table S3. The geometrical parameters (in Å and degree) of the transition states of $FNgPbF_3$ for the dissociation resulting in the formation of PbF_2 and NgF_2 studied at the MP2/def2-TZVPPD level.

	Clusters	$r_{F\text{-}Ng}$	$r_{F(bridge)\text{-}Ng}$	$r_{Ng\text{-}Pb}$	$r_{F(bridge)\text{-}Pb}$	$r_{Pb\text{-}F}$	<FNgF	<F(bridge)PbNg
Transition	$FXePbF_3$	2.024	2.547	3.042	2.124	2.013, 2.027	150.2	55.7
State	$FRnPbF_3$	2.077	2.627	3.056	2.121	2.016	147.3	57.6

Table S4. Harmonic vibrational frequencies ($\tilde{\nu}$, cm^{-1}) and the corresponding IR intensities (km/mol) calculated at the MP2/def2-TZVPPD level.

Clusters	**$\tilde{\nu}$ (F-Ng)**	**$\tilde{\nu}$ (Ng-Sn)**	**$\tilde{\nu}$ (Sn-F)**	**δ (F-Ng-Sn)**	**δ (Ng-Sn-F)**	**δ (F-Sn-F)**	**Umbrella (SnF_3)**
$FKrSnF_3$	452 (388/a_1)	136 (68/a_1)	644 (128/a_1) 667 (90/e)	58 (11/e)	144 (9/e)	172 (7/e)	214 (55/a_1)
$FXeSnF_3$	447 (325/a_1)	140 (33/a_1)	646 (111/a_1) 662 (89/e)	62 (11/e)	134 (6/e)	171 (10/e)	213 (69/a_1)
$FRnSnF_3$	451 (294/a_1)	130 (23/a_1)	644 (115/a_1) 658 (89/e)	61 (11/e)	121 (4/e)	171 (11/e)	213 (72/a_1)
FKrSnF	331 (326/a')	177 (65/a')	624 (106/a')	61 (14/a")	63 (15/ a')		
FXeSnF	345 (363/a')	167 (34/a')	609 (105/a')	65 (12/a")	66 (12/ a')		
FRnSnF	353 (352/a')	157 (22/a')	603 (105/a')	61 (11/a")	62 (12/ a')		

Table S5. Harmonic vibrational frequencies ($\tilde{\nu}$, cm^{-1}) and the corresponding IR intensities (km/mol) calculated at the MP2/def2-TZVPPD level. (Ng-Pb)

Clusters	**$\tilde{\nu}$ (F-Ng)**	**$\tilde{\nu}$ (Ng-Pb)**	**$\tilde{\nu}$ (Pb-F)**	**δ (F-Ng-Pb)**	**δ (Ng-Pb-F)**	**δ (F-Pb-F)**	**Umbrella (PbF_3)**
$FKrPbF_3$	469 (10/a_1)	108 (18/a_1)	549 (175/a_1) 559 (85/e)	28 (7/e)	123 (8/e)	136 (2/e)	151 (25/a_1)
$FXePbF_3$	461 (281/a_1)	124 (19/a_1)	566 (119/a_1) 569 (87/e)	38 (9/e)	124 (7/e)	141 (4/e)	158 (34/a_1)
$FRnPbF_3$	468 (298/a_1)	115 (14/a_1)	569.8 (88/e) 570.2 (112/ a_1)	37 (9/e)	112 (5/e)	141 (7/e)	160 (39/a_1)
FKrPbF	320 (347/a')	154 (52/a')	564 (107/a')	59 (15/a")	59 (15/ a')		
FXePbF	336 (388/a')	141 (25/a')	550 (105/a')	63 (12/a")	61 (12/ a')		
FRnPbF	346 (372/a')	130 (16/a')	544 (104/a')	59 (12/a")	59 (11/ a')		

Harmonic vibrational frequencies

In order to recognize the signature of a particular bond in the IR spectrum, the knowledge of the IR frequencies and IR intensities associated with that bond is essential. Hence, we have tabulated the IR frequencies and intensities corresponding to different harmonic vibrational modes (see Tables S4 and S5). In $FNgSnF_3$ compounds, the F-Ng stretching frequency values are in the range of 447-452 cm^{-1} in which the F-Kr (452 cm^{-1}) and F-Rn (451 cm^{-1}) show almost same stretching frequency whereas the same for F-Xe is slightly less (447 cm^{-1}). This F-Ng stretching mode exhibits the most intense peak among all the vibrational modes having a range in between 294 and 388 km/mol. The intensity somewhat reduces in moving from Kr to Rn. The Ng-Sn stretching frequency ranges in between 130 to 140 cm^{-1}, with the highest value for Xe-Sn. Though less intense

than F-Ng, these Ng-Sn stretching modes are also IR active having intensity in the range of 23-68 km/mol with Kr-Sn having the most intense and Rn-Sn having the least intense peaks.

The stretching frequency value of Sn-F bond is the largest (range 644-667 cm^{-1}) among the other stretching modes of a given $FNgSnF_3$ compound. The doubly degenerate e component of Sn-F stretching is less intense (range 89-90 km/mol) than that of a_1 component (range 111-128 km/mol). The frequencies of F-Ng-Sn and Ng-Sn-F bending modes lie in the range of 58-62 and 121-144 cm^{-1}, respectively. Both the bending modes are very less intense (4-11 km/mol). The less intense F-Sn-F bending motion occurs at around 171 cm^{-1} whereas the so-called 'umbrella' motion of SnF_3 occurs at around 213 cm^{-1}, which is comparatively more intense (range 55-72 km/mol).

Now, in cases of FNgSnF compounds the frequency for F-Ng stretching lies in between 331-353 cm^{-1} with intensity in the range of 326 to 363 km/mol. Note that similar to $FNgSnF_3$, this mode exhibits the most intense peak for a given FNgSnF compound. The Sn-F stretching frequency (range 603-624 cm^{-1}) is higher and more intense (range 105-106 km/mol) than that of Ng-Sn stretching (frequency range 157-177 cm^{-1} and intensity range 22-65 km/mol). Note that both the frequency values and intensities for the Ng-Sn stretching decrease gradually in moving from Kr to Rn. Both, F-Ng-Sn and Ng-Sn-F bending modes are found to be very less intense (11-15 km/mol) and they have very similar frequency values (61-66 cm^{-1}).

In $FNgPbF_3$ compounds, the F-Ng stretching frequency values are in the range of 461-469 cm^{-1} in which F-Xe and F-Rn stretching modes exhibit the most intense peaks (281 km/mol in Xe and 298 km/mol in Rn) in their respective spectra. However, the F-Kr stretching mode is less intense (10 km/mol). The Ng-Pb stretching frequency ranges in between 108 and 124 cm^{-1}, having the highest value for Xe-Pb. The Ng-Pb stretching modes exhibit quite less intense peaks having intensity in the range of 14-18 km/mol. The frequency values corresponding to the Pb-F stretching modes lie in between 549-570 cm^{-1}, which have intensity in the range of 85-175 km/mol. The a_1 component of Pb-F stretching is more intense than that of e component. In $FKrPbF_3$, the a_1 component of Pb-F stretching exhibits the most intense peak in the spectrum. The F-Ng-Pb, Ng-Pb-F and F-Pb-F bending modes display much less intense peaks (range 2-9 km/mol) and have

frequencies in the range of 28-38, 112-124 and 136-141 cm^{-1}, respectively. The 'umbrella' motion of PbF_3 takes place in the range of 151-160 cm^{-1} having intensity of 25-39 km/mol. The F-Ng stretching frequencies in FNgPbF compounds lie in between 320-346 cm^{-1} with intensity in the range of 347 to 388 km/mol. This mode corresponds to the most intense peak in the spectrum. The Pb-F stretching mode (544-564 cm^{-1}) has higher IR intensity than that of Ng-Pb stretching (130-154 cm^{-1}). All the bending modes are much less intense (11-15 km/mol).

Table S6. The interaction energy (ΔE_{int}, kcal/mol) and dissociation energy (D_e, kcal/mol) computed at the MP2/def2-TZVPPD level. The preparation energy values (in kcal/mol) of each fragment are given within parentheses.

Systems	Fragments	ΔE_{int}	D_e
$FKrSnF_3$	F^- + $[KrSnF_3]^+$ (0.0) (12.2)	-148.5	136.2
	[FKr] + $[SnF_3]$ (15.7) (0.3)	-24.8	8.8
$FXeSnF_3$	F^- + $[XeSnF_3]^+$ (0.0) (10.2)	-161.8	151.6
	[FXe] + $[SnF_3]$ (5.3) (0.1)	-38.2	32.8
$FRnSnF_3$	F^- + $[RnSnF_3]^+$ (0.0) (9.4)	-168.7	159.3
	[FRn] + $[SnF_3]$ (0.2) (0.0)	-44.2	44.0
FKrSnF	F^- + $[KrSnF]^+$ (0.0) (5.3)	-101.5	96.1
	$[FKr]^-$ + $[SnF]^+$ (16.0) (0.5)	-116.9	100.3
	[FKr] + [SnF] (7.6) (0.3)	-33.3	25.5

FXeSnF	F^- (0.0) + $[XeSnF]^+$ (3.9)	-111.6	107.6
	$[FXe]^-$ (16.5) + $[SnF]^+$ (0.5)	-116.9	100.3
	[FXe] (4.5) + [SnF] (0.1)	-45.3	40.6
FRnSnF	F^- (0.0) + $[RnSnF]^+$ (2.8)	-117.0	114.1
	$[FRn]^-$ (14.4) + $[SnF]^+$ (0.9)	-136.6	121.2
	[FRn] (2.5) + [SnF] (0.1)	-49.8	47.2

Table S7. The interaction energy (ΔE_{int}, kcal/mol) and dissociation energy (D_e, kcal/mol) computed at the MP2/def2-TZVPPD level. The preparation energy values (in kcal/mol) of each fragment are given within parentheses.

Systems	Fragments	ΔE_{int}	D_e
$FKrPbF_3$	F^- (0.0) + $[KrPbF_3]^+$ (16.3)	-166.0	149.7
	[FKr] (16.0) + $[PbF_3]$ (0.3)	-17.2	0.9
$FXePbF_3$	F^- (0.0) + $[XePbF_3]^+$ (12.2)	-176.8	164.5
	[FXe] (5.6) + $[PbF_3]$ (0.6)	-30.5	24.2
$FRnPbF_3$	F^- (0.0) + $[RnPbF_3]^+$ (10.7)	-183.5	172.8
	[FRn] (0.0) + $[PbF_3]$ (0.8)	-37.1	36.3
FKrPbF	F^- + $[KrPbF]^+$	-97.7	93.0

	(0.0) (4.7)		
	$[FKr]^-$ + $[PbF]^+$ (14.6) (0.5)	-112.9	97.8
	[FKr] + [PbF] (7.0) (0.3)	-34.2	26.9
FXPbF	F^- + $[XePbF]^+$ (0.0) (3.6)	-107.8	104.3
	$[FXe]^-$ + $[PbF]^+$ (15.5) (0.8)	-126.6	110.4
	[FXe] + [PbF] (4.4) (0.2)	-46.3	41.7
FRnPbF	F^- + $[RnPbF]^+$ (0.0) (2.6)	-113.6	110.9
	$[FRn]^-$ + $[PbF]^+$ (13.8) (0.9)	-132.8	118.1
	[FRn] + [PbF] (2.6) (0.1)	-50.9	48.2

Table S8. The geometrical parameters (in Å and degree) of the optimized structures of $FXeEF_3$ and FXeEF clusters (E = Ge, Sn) studied at the MP2/def2-TZVPPD level.

	Clusters	r_{F-Xe}	r_{Xe-E}	r_{E-F}	<FXeE	<XeEF
	$FXeGeF_3$	2.114	2.564	1.707	180.0	111.5
	$FXeSnF_3$	2.102	2.755	1.892	180.0	112.7
	$FXePbF_3$	2.069	2.852	2.002	180.0	114.8
Minima	FXeGeF	2.246	2.673	1.736	179.8	95.1
	FXeSnF	2.271	2.852	1.926	179.8	93.4
	FXePbF	2.285	2.921	2.032	179.0	94.3
	$FXeGeF_3$	2.382	2.466	1.683, 1.691	101.4	107.4, 109.1
	$FXeSnF_3$	2.384	2.627	1.865, 1.874	101.7	108.0, 108.8
	$FXePbF_3$	2.387	2.698	1.962, 1.975	99.2	108.4, 109.3
TSs	FXeGeF	2.372	2.608	1.726	107.5	96.2
	FXeSnF	2.399	2.792	1.918	112.0	94.8
	FXePbF	2.413	2.869	2.024	114.7	96.9

Table S9. ZPE corrected dissociation energy (D_0, kcal/mol), dissociation enthalpy (ΔH, kcal/mol) and free energy change (ΔG, kcal/mol) for different dissociation channels of $FXeEF_3$ and FXeEF clusters (E = Ge, Sn) at the MP2/def2-TZVPPD level.

Processes	D_0			ΔH			ΔG		
	Ge	Sn	Pb	Ge	Sn	Pb	Ge	Sn	Pb
$FXeEF_3 \rightarrow F + Xe + EF_3$	38.6	31.8	23.2	39.3	32.4	23.8	22.7	16.3	8.0
$FXeEF_3 \rightarrow XeF_2 + EF_2$	55.0	31.3	-10.0	55.1	31.0	-10.5	44.9	21.6	-19.1
$FXeEF_3 \rightarrow F^- + XeEF_3^+$	150.4	150.9	163.7	150.9	151.3	164.1	142.9	143.3	156.3
$FXeEF_3 \rightarrow Xe + EF_4$	-95.6	-81.1	-53.5	-95.7	-81.2	-53.6	-101.7	-87.2	-59.4
$\Delta E^{\ddagger a}$	31.2	32.7	46.6						
$FXeEF \rightarrow F + Xe + EF$	38.7	40.0	41.1	39.5	40.6	41.7	25.2	26.7	27.9
$FXeEF \rightarrow XeF_2 + E$	131.6	120.5	113.9	131.7	120.4	113.8	126.9	116.1	109.7
$FXeEF \rightarrow F^- + XeEF^+$	113.6	106.9	103.6	114.0	107.3	103.9	106.1	99.5	96.2
$FXeEF \rightarrow Xe + EF_2$	-100.6	-90.1	-80.5	-100.7	-90.2	-80.6	-106.8	-96.3	-86.7
$\Delta E^{\ddagger b}$	8.7	6.9	6.0						

$\Delta E^{\ddagger a}$ is the activation barrier for the process $FXeEF_3 \rightarrow Xe + EF_4$; $\Delta E^{\ddagger b}$ is the activation barrier for the process $FXeEF \rightarrow Xe + EF_2$

Table S10. NPA charge on each atomic center (q_k, au) and WBI values of F-Xe and Ng-E (E = Ge, Sn) bonds computed at the MP2/def2-TZVPPD level.

Clusters	**q_k**				**WBI**	
	F(Xe)	**Xe**	**E**	**F(E)**	**F-Xe**	**Xe-E**
$FXeGeF_3$	-0.831	+0.707	+2.236	-0.704	0.305	0.720
$FXeSnF_3$	-0.816	+0.688	+2.381	-0.751	0.197	0.794
$FXePbF_3$	-0.737	+0.822	+2.142	-0.742	0.275	0.722
FXeGeF	-0.909	+0.418	+1.268	-0.777	0.109	0.711
FXeSnF	-0.921	+0.367	+1.371	-0.817	0.098	0.618
FXePbF	-0.926	+0.334	+1.421	-0.829	0.092	0.573

Table S11. Electron density descriptors (au) at the bond critical points (BCP) obtained from the wave functions generated at the MP2/def2-TZVPPD/WTBS level (WTBS for Pb, Xe and Rn atoms) taking optimized geometries at the MP2/def2-TZVPPD level.

Clusters	BCP	$\rho(r_c)$	$\nabla^2\rho(r_c)$	$G(r_c)$	$V(r_c)$	$H(r_c)$	$G(r_c)/\rho(r_c)$	Class	r_{cov}	r_e
$FXeGeF_3$	F-Xe	0.087	0.282	0.095	-0.120	-0.025	1.092	W[c]	1.97[a]/1.95[b]	2.11
	Xe-Ge	0.084	-0.033	0.029	-0.066	-0.037	0.345	C	2.60[a]/2.52[b]	2.56
$FXeSnF_3$	F-Xe	0.090	0.290	0.099	-0.125	-0.026	1.100	W[c]	1.97[a]/1.95[b]	2.10
	Xe-Sn	0.054	0.041	0.024	-0.037	-0.013	0.444	C	2.79[a]/2.71[b]	2.76
$FXePbF_3$	F-Xe	0.096	0.305	0.107	-0.137	-0.030	1.115	W[c]	1.97[a]/1.95[b]	2.07
	Xe-Pb	0.049	0.054	0.024	-0.034	-0.010	0.490	C	2.86[a]/2.75[b]	2.85
FXeGeF	F-Xe	0.068	0.248	0.075	-0.088	-0.013	1.103	W[c]	1.97[a]/1.95[b]	2.25
	Xe-Ge	0.069	-0.020	0.023	-0.051	-0.028	0.333	C	2.60[a]/2.52[b]	2.67
FXeSnF	F-Xe	0.065	0.245	0.072	-0.083	-0.011	1.108	W[c]	1.97[a]/1.95[b]	2.27
	Xe-Sn	0.043	0.055	0.022	-0.030	-0.008	0.512	C	2.79[a]/2.71[b]	2.85
FXePbF	F-Xe	0.064	0.241	0.070	-0.081	-0.011	1.094	W[c]	1.97[a]/1.95[b]	2.29
	Xe-Pb	0.041	0.066	0.023	-0.029	-0.006	0.561	C	2.86[a]/2.75[b]	2.92

The Cartesian coordinates of the minimum energy and transition state structures of $FNgEF_3$ and FNgEF compounds at the MP2/def2-TZVPPD level

Minimum energy structure	Transition state for $FNgEF_n$ □ $\rightarrow$ Ng + $EF_{(n+1)}$
0 1 Sn 0.00000000 0.00000000 0.95960800	0 1 Sn 0.38100600 0.77970600 0.00000000

F	0.00000000	1.75536100	1.65941300	F	-0.29134000	1.49802200	1.57687800
F	1.52018700	-0.87768100	1.65941300	F	-0.29134000	1.49802200	-1.57687800
F	-1.52018700	-0.87768100	1.65941300	F	2.24917300	0.81238500	0.00000000
F	0.00000000	0.00000000	-3.68227400	F	-2.61783300	-1.75049800	0.00000000
Kr	0.00000000	0.00000000	-1.65678000	Kr	-0.29134000	-1.59740800	0.00000000
$FKrSnF_3$				$FKrSnF_3$			
0 1				0 1			
Sn	0.00000000	0.00000000	-1.23431700	Sn	0.41659100	1.02860200	0.00000000
F	0.00000000	1.74598300	-1.96414500	F	-0.24652400	1.79823900	1.56432000
F	-1.51206600	-0.87299200	-1.96414500	F	-0.24652400	1.79823900	-1.56432000
F	1.51206600	-0.87299200	-1.96414500	F	2.28567500	1.16565100	0.00000000
Xe	0.00000000	0.00000000	1.52108800	F	-2.62787500	-1.39388200	0.00000000
F	0.00000000	0.00000000	3.62322100	Xe	-0.24652400	-1.51378400	0.00000000
$FXeSnF_3$				$FXeSnF_3$			
0 1				0 1			
Sn	0.00000000	0.00000000	-1.55668100	Sn	0.45562200	-1.33897200	0.00000000
F	0.00000000	1.74055800	-2.30526000	F	1.45956700	-1.55958900	1.56015400
F	-1.50736800	-0.87027900	-2.30526000	F	1.45956700	-1.55958900	-1.56015400
F	1.50736800	-0.87027900	-2.30526000	F	-0.90974600	-2.62742900	0.00000000
F	0.00000000	0.00000000	3.42727300	F	1.45956700	2.36455400	0.00000000
Rn	0.00000000	0.00000000	1.27012400	Rn	-0.62792700	1.13240800	0.00000000
$FRnSnF_3$				$FRnSnF_3$			
0 1				0 1			
Sn	0.31785400	-1.31317200	0.00000000	Sn	1.22040100	0.35273800	0.01202200
F	-1.56839200	-1.65089600	0.00000000	F	1.69072800	-1.42524600	0.52929300
F	-0.19746300	3.57530700	0.00000000	F	-3.14788100	0.38136800	0.97383200
Kr	0.00000000	1.34274700	0.00000000	Kr	-1.33071300	-0.22894500	-0.39247900
FKrSnF				FKrSnF			
0 1				0 1			
Sn	0.32822500	-1.60474600	0.00000000	Sn	1.46845300	0.24227800	-0.25160500
F	-1.56856800	-1.94018700	0.00000000	F	1.90300300	-0.53277800	1.44783800
Xe	0.00000000	1.22837400	0.00000000	F	-2.56932800	1.49771000	0.57931100
F	-0.25490600	3.48520300	0.00000000	Xe	-1.24862400	-0.38515300	-0.10489000
FXeSnF				FXeSnF			
0 1				0 1			
Sn	0.33213800	-1.90991200	0.00000000	Sn	1.76140600	0.18755500	-0.29025500
F	-1.56931200	-2.24470500	0.00000000	F	2.18756700	-0.31706000	1.51407700
F	-0.27589900	3.29149200	0.00000000	F	-2.03503300	1.90521500	0.37129300
Rn	0.00000000	1.00086600	0.00000000	Rn	-1.04003600	-0.27524600	-0.02855300
FRnSnF				FRnSnF			
0 1				0 1			
F	0.00000000	1.83573400	1.60829200	F	-1.11659100	0.87621900	1.67863700
F	1.58979200	-0.91786700	1.60829200	F	-1.11659100	0.87621900	-1.67863700
F	-1.58979200	-0.91786700	1.60829200	F	1.44024700	1.87306600	0.00000000
F	0.00000000	0.00000000	-4.02456000	F	-1.11659100	-3.09095900	0.00000000
Pb	0.00000000	0.00000000	0.79223700	Kr	0.78132200	-1.70429500	0.00000000
Kr	0.00000000	0.00000000	-2.00462000	Pb	-0.13343700	0.68955800	0.00000000
$FKrPbF_3$				$FKrPbF_3$			

0 1 F 0.00000000 1.81772900 1.86070600 F 1.57419900 -0.90886400 1.86070600 F -1.57419900 -0.90886400 1.86070600 Xe 0.00000000 0.00000000 -1.83089700 F 0.00000000 0.00000000 -3.89953200 Pb 0.00000000 0.00000000 1.02103800 $FXePbF_3$	0 1 F -0.32874600 1.68923800 1.64672100 F -0.32874600 1.68923800 -1.64672100 F 2.30254400 0.99571800 0.00000000 F -2.70690600 -1.55729700 0.00000000 Xe -0.32874600 -1.76329800 0.00000000 Pb 0.33303600 0.85202500 0.00000000 $FXePbF_3$
0 1 F 0.00000000 1.80935500 -2.18726000 F -1.56694700 -0.90467700 -2.18726000 F 1.56694700 -0.90467700 -2.18726000 F 0.00000000 0.00000000 3.69060500 Rn 0.00000000 0.00000000 1.56881500 Pb 0.00000000 0.00000000 -1.33021400 $FRnPbF_3$	0 1 F -0.27119300 2.02437700 1.63435000 F -0.27119300 2.02437700 -1.63435000 F 2.34743500 1.34230500 0.00000000 F -2.66400500 -1.16997500 0.00000000 Rn -0.27119300 -1.53376100 0.00000000 Pb 0.37869800 1.14528900 0.00000000 $FRnPbF_3$
0 1 F 2.02052700 1.00046300 0.00000000 F -0.73005800 -3.90406000 0.00000000 Kr -0.32261700 -1.67833300 0.00000000 Pb 0.00000000 1.05551700 0.00000000 FKrPbF	0 1 F 1.56447600 -1.60031200 0.50989500 F -3.59226100 0.51312300 0.82325600 Kr -1.69116000 -0.31038500 -0.32435200 Pb 0.96502200 0.25559200 -0.00392300 FKrPbF
0 1 F 2.03165800 1.30068100 0.00000000 Xe -0.25580600 -1.58548100 0.00000000 F -0.49682400 -3.85804100 0.00000000 Pb 0.00000000 1.32478300 0.00000000 FXePbF	0 1 F 1.69271600 -1.28667000 1.15547000 F -2.99944100 1.17521400 1.04624400 Xe -1.60839100 -0.33018600 -0.22708800 Pb 1.20260500 0.22967300 -0.09210600 FXePbF
0 1 F 1.80140700 -1.90706300 0.00000000 F 0.16220600 3.67392200 0.00000000 Rn 0.00000000 1.36222400 0.00000000 Pb -0.21551900 -1.62259700 0.00000000 FRnPbF	0 1 F 1.95224800 -0.90371500 1.49311500 F -2.44286300 1.74751800 0.79453900 Pb 1.50321800 0.18515200 -0.15731700 Rn -1.38195700 -0.26484500 -0.08940600 FRnPbF

The coordinates of the transition states of $FNgPbF_3$ for the dissociation channel, $FNgPbF_3 \rightarrow NgF_2 + PbF_2$

0 1 F -0.05970000 -0.83639500 1.43983000 F -2.92870500 -0.94476800 -0.16046900 F -1.66736700 1.79883400 0.62244500 Xe 1.88338400 -0.04552700 -0.00366700 F 3.87194200 0.19732900 -0.29336000 Pb -1.15424700 0.00638400 -0.17412200 $FXePbF_3$	0 1 F -0.39602500 0.00089000 1.68980500 F -2.73410000 -1.53875200 0.03529000 F -2.73521900 1.53785200 0.03429600 F 3.66700600 -0.00020800 -0.28167900 Pb -1.44491600 -0.00000100 -0.15346000 Rn 1.60777000 0.00002400 -0.00832200 $FRnPbF_3$

The Cartesian coordinates of the minimum energy structures of FNgEF compounds at the CCSD(T)/def2-TZVP level

0 1 Sn -1.33847000 -0.29604000 0.00043600 F -1.64096700 1.59479500 0.00005400 F 3.57804200 0.15753800 0.00305800 Kr 1.37471800 -0.02691600 -0.00138400 FKrSnF	0 1 Sn -0.32661000 -1.62405600 0.00000000 F 1.56753300 -1.95479400 0.00000000 Xe 0.00000000 1.24963200 0.00000000 F 0.24696800 3.47953700 0.00000000 FXeSnF
0 1 Sn -0.33050700 -1.93386200 0.00000000 F 1.56764600 -2.26397800 0.00000000 F 0.26850500 3.28508000 0.00000000 Rn 0.00000000 1.01747900 0.00000000 FRnSnF	0 1 F 2.02921400 1.27997400 0.00000000 Xe -0.25621800 -1.61043900 0.00000000 F -0.49190600 -3.85735700 0.00000000 Pb 0.00000000 1.34341700 0.00000000 **FXePbF**
0 1 F 1.80297200 -1.90414300 0.00000000 F 0.15802500 3.67294900 0.00000000 Rn 0.00000000 1.38356800 0.00000000 Pb -0.21523100 -1.64519600 0.00000000 FRnPbF	